

# The energy-momentum tensor in a classical model of the electron

Grace Gardella<sup>1,2</sup>, Mira Varma<sup>3,2</sup>, Peter Schweitzer<sup>2</sup>

<sup>1</sup> *Department of Physics, Illinois Institute of Technology, Chicago, Illinois 60616-3793, USA*

<sup>2</sup> *Department of Physics, University of Connecticut, Storrs, CT 06269-3046, USA*

<sup>3</sup> *Department of Physics, Yale University, New Haven, CT 06520, USA*

(Dated: March 2026)

We show that the leading non-analytic terms in the small- $t$  expansion of the energy momentum tensor (EMT) form factors of an electrically charged particle in QED can be correctly derived in a classical model of the electron by Białynicki-Birula. Based on the lucidity of the employed exactly solvable model, we comment also on the recently proposed concept of a regularized proton  $D$ -term.

## I. INTRODUCTION

Form factors of the energy-momentum tensor (EMT) have attracted considerable attention in the recent past. The EMT matrix elements give access to fundamental particle properties including the mass [1], spin [2] and  $D$ -term [3] with significant potential for new insights in hadron structure [4–9]. In theoretical studies of hadrons, the focus is naturally on the short-range strong forces. Electromagnetic effects, often deemed to play no major role for hadron structure, are rarely considered in such studies. In systems governed by short-range forces one finds a negative EMT form factor  $D(t)$  which has a regular limit  $D = \lim_{t \rightarrow 0} D(t)$  known as the  $D$ -term.<sup>1</sup>

The presence of electromagnetic or other long-range forces affects the EMT properties strongly. In particular, the form factor  $D(t)$  of a charged particle develops a  $1/\sqrt{-t}$  singularity and the  $D$ -term is undefined as was observed for the electron in QED [19, 20], charged pions in chiral perturbation theory [21], in computations of quantum gravitational corrections for charged spin-0 and spin- $\frac{1}{2}$  particles [22] and proton [23, 24]. The electron EMT was recently further investigated in [25, 26]. Other systems with long-range forces were discussed in [27–30]. The goal of this work is to present a study of the EMT properties in the classical electron model constructed by Białynicki-Birula in [32].

Since the discovery of the electron by Thomson in 1897 [31], numerous efforts were made to construct classical models of extended, charged particles with contributions by Thomson, Abraham, Lorentz, Poincaré, Einstein, Wien, Planck, Sommerfeld, Langevin, Ehrenfest, Born, Pauli, von Laue and others [32]. Even after quantum mechanics superseded classical physics in the 1920s, the formulation of consistent classical models of finite-size charged particles remained an intellectual challenge and continues attracting interest to this day [32–38].

In the model of Białynicki-Birula, the electron is made of a “perfect, charged fluid and the electromagnetic field” [32]. The model was introduced to help resolve a controversy in literature between Boyer and Rohrlich on how to consistently calculate the electromagnetic energy and momentum of a classical moving charged particle [38, 39]. In this work we will explore the model to study the EMT properties of the electron. Several features make this model an attractive choice for our purposes. (i) The model describes a finite-size electrically charged particle in a theoretically consistent and relativistic way. (ii) The cohesive forces which bind the system are included in the “internal dynamics of the system” [32]. (iii) The simplicity of the model will allow us to compute the EMT properties analytically and present lucid interpretations of the results. In this model, the electron has a finite radius which in principle can be fixed to be smaller than the experimental upper bounds for size of the electron, but in this work we will refrain from fixing parameters and focus on analytical results.

It is expected that results from classical electrodynamics and QED should coincide in the long-distance limit [22]. The goal of this work is to test this expectation. After introducing the model in Sec. II, we will study the spatial distribution related to the energy density and the stress tensor distributions in Sec. III, and compute the form factors  $A(t)$  and  $D(t)$  in the model in Sec. IV, which will include a study of the limits four-momentum transfer  $t \rightarrow 0$  and  $R \rightarrow 0$  to restore a pointlike electron. As an interesting byproduct, we will explore the model in Sec. V to shed some light on the concept of a “regularized  $D$ -term” proposed for the proton [23, 24]. In Sec. VI we present the conclusions.

---

<sup>1</sup> The form factor  $D(t)$  [3] has attracted a lot of interest also due to its appealing interpretation in terms of mechanical properties [10], see the reviews [11, 12]. The interpretation was elaborated in [13, 14] and encountered also some criticism in literature [15–17]. In this work we use the interpretation in a “reversed direction” as a practical tool for our calculations and demonstrate that we obtain correct results. This is not intended to resolve any controversy, but it speaks for itself: when applied responsibly within its limitation, the 3D interpretation yields correct results for form factors. This is how Hofstadter used the 3D interpretation in his seminal works [18].

## II. THE CLASSICAL MODEL OF THE ELECTRON

In this section, we introduce the classical electron model [32]. In this model, the electron is made of a perfect charged fluid and the electromagnetic field. The energy momentum tensor (EMT) of the system is given by [32]

$$T^{\mu\nu} = (\rho_{\text{fluid}} + p_{\text{fluid}})u^\mu u^\nu + \frac{1}{4\pi}F^\mu{}_\lambda F^{\lambda\nu} - g^{\mu\nu} \frac{1}{16\pi}F_{\alpha\beta}F^{\alpha\beta}, \quad (1)$$

where  $\rho_{\text{fluid}}$  and  $p_{\text{fluid}}$  are the mass-energy density and pressure of the fluid and  $u^\mu$  is its four-velocity, while  $F^{\mu\nu}$  is the electromagnetic field strength tensor. The flow of the fluid is adiabatic, and  $\rho_{\text{fluid}}$  and  $p_{\text{fluid}}$  as functions of the scalar fluid density  $n$  obey the relation

$$\frac{d\rho_{\text{fluid}}}{dn} = \frac{\rho_{\text{fluid}} + p_{\text{fluid}}}{n}. \quad (2)$$

The equations of motion describing the perfect charged fluid coupled to the electromagnetic field are given by

$$(a) \quad qn F^{\alpha\nu}u_\alpha + (\partial^\nu - u^\nu u^\mu \partial_\mu)p_{\text{fluid}} = (\rho_{\text{fluid}} + p_{\text{fluid}})u^\mu \partial_\mu u^\nu, \quad (b) \quad \partial_\mu F^{\mu\nu} = 4\pi qn u^\nu \quad (3)$$

where  $qn u^\mu$  is the four-current density with  $q$  the electron charge.<sup>2</sup> In the rest frame of the system, the fluid is described by a static configuration and  $u^\mu = (1, 0, 0, 0)$  such that the equations of motion in Eq. (3) become

$$(a) \quad qn \vec{E} - \vec{\nabla} p_{\text{fluid}} = 0, \quad (b) \quad \vec{\nabla} \cdot \vec{E} = 4\pi qn. \quad (4)$$

In order to overcome the repulsion within the fluid and form a stable and bound system, the following equation of state was imposed in the model where  $\kappa$  is a positive constant [32],

$$p_{\text{fluid}}(n) = -\kappa n^{6/5}. \quad (5)$$

The negative sign in Eq. (5) indicates that this pressure is a Poincaré stress, i.e. provides the cohesive force which is responsible for binding the system [40]. Based on the equation of state (5), the adiabatic flow equation (2) yields

$$\rho_{\text{fluid}}(r) = m_{\text{fluid}} n(r) - 5\kappa n(r)^{6/5} \quad (6)$$

where  $m_{\text{fluid}}$  is an integration constant due to solving Eq. (2) with the meaning of the mechanical mass of the system, i.e. the mass the perfect fluid would have if it was not subject to electromagnetic forces and the equation of state (5). The solution of the static equations of motion in Eq. (4) is then given by

$$\vec{E}(\vec{r}) = E(r) \vec{e}_r, \quad E(r) = \frac{qr}{(R^2 + r^2)^{3/2}}, \quad (7)$$

$$n(r) = \frac{3}{4\pi} \frac{R^2}{(R^2 + r^2)^{5/2}}, \quad R^2 = \frac{4\pi}{3} \left( \frac{q^2}{6\kappa} \right)^5, \quad (8)$$

where  $r = |\vec{r}|$  and  $\vec{e}_r = \vec{r}/r$ . The parameter  $R > 0$  characterizes the size of the system and can be referred to as the “electron radius” [32]. Notice that the scalar density is normalized as  $\int d^3r n(r) = 1$  and Eq. (4a) is satisfied only for the value of  $R$  quoted in Eq. (8) while Eq. (4b) holds for any  $R$ .

---

<sup>2</sup> We use Gauss units where the Coulomb force between two static charges  $q_i$  is  $F = \frac{q_1 q_2}{r^2}$  and natural units with  $c = \hbar = 1$ . In this unit system, the fine structure constant  $\alpha = q^2 \simeq \frac{1}{137}$ , i.e. the electron charge is given by  $q = -\sqrt{\alpha}$ .

### III. THE SPATIAL EMT DISTRIBUTIONS IN THE ELECTRON MODEL

After the preparations in Sec. II, we are now in the position to study the EMT properties of the electron in the classical model. In the following, we evaluate the components of the EMT in Eq. (1) in the rest frame of the system.

#### A. Energy density $T_{00}(r)$

Inserting in Eq. (1) the solutions (7, 8) we obtain for the energy density the result

$$T_{00}(r) = \rho_{\text{fluid}}(r) + \frac{1}{8\pi} E(r)^2 = \frac{1}{8\pi} \left[ \frac{6m_{\text{fluid}}R^2}{(r^2 + R^2)^{5/2}} + \frac{\alpha r^2}{(r^2 + R^2)^3} - \frac{\lambda_p \alpha R^2}{(r^2 + R^2)^3} \right] \quad (9)$$

where we used the fine structure constant  $\alpha = q^2$  (see footnote 2 on units), and eliminated  $\kappa$  by means of Eq. (8). The latter step renders the model expressions elegant but makes it difficult to tell apart the terms of electromagnetic origins and those due to Poincaré stress in Eq. (5). We therefore introduce the constant

$$\lambda_p = 1 \quad (10)$$

to label the contribution due to the Poincaré stress. The advantage of introducing  $\lambda_p$  becomes immediately apparent when we compute the mass of the system,

$$M = \int d^3r T_{00}(r) = m_{\text{fluid}} + \frac{3\pi\alpha}{32R} - \lambda_p \frac{5\pi\alpha}{32R}, \quad (11)$$

where we see in detail how  $M$  arises: the mechanical mass  $m_{\text{fluid}}$  is augmented by the electromagnetic contribution  $\frac{3\pi\alpha}{32R}$  because the electric field of the charge configuration carries energy, and is diminished by  $-\lambda_p \frac{5\pi\alpha}{32R}$  due to the Poincaré stress which provides the binding effect. Inserting  $\lambda_p = 1$  we see that the system is ultimately bound

$$M = m_{\text{fluid}} + E_{\text{bind}} < m_{\text{fluid}}, \quad E_{\text{bind}} = -\frac{\pi\alpha}{16R} < 0. \quad (12)$$

So far the electron appears point-like in experiments. The determinations of experimental upper bounds on its size are in general model dependent, see for example [41–45]. For instance, the upper bound for the electron radius derived from data obtained from Large Electron-Positron (LEP) collider experiments is  $R_{\text{exp}} < 3.1 \times 10^{-19}\text{m}$  at a 95% confidence level [44]. If we would set the model parameter  $R = 10^{-20}\text{m}$  within experimental limits, then the electron mass arises from significant cancellations,

$$M = 28,234.715 \text{ MeV} + 42,351.306 \text{ MeV} - 70,585.510 \text{ MeV} = 0.511 \text{ MeV}, \quad (13)$$

with the different contributions quoted in the order of their appearance in Eq. (11). Notice that the physical mass is nearly negligible compared to the other numbers in Eq. (13), and to a good approximation  $m_{\text{fluid}} \simeq \frac{\pi\alpha}{16R} = |E_{\text{bind}}|$ .

A realistic description of the electron substructure, if there was any, would of course require quantum field theoretical compositeness models. The point is that one can choose  $R$  small enough for the model to not contradict experimental results. For  $r \lesssim R$  the results are model dependent, but in the long-distance limit  $r \gg R$  we will be able to use this classical framework to obtain model-independent results and confirm QED predictions. In the following, we will not need to fix the parameters and will focus on analytical results.

In Fig. 1a we show  $T_{00}(r)$  in units of  $M/R^3$  plotted as function of  $r$  in units of  $R$ . As can be seen in Fig. 1a, the electron is a diffuse object in the model: 50% of its mass is contained within a radius of  $r \leq 1.3R$ ; and 80% within  $r \leq 2.5R$ . Comparing  $T_{00}(r)$  to the charge distribution  $\rho_{el}(r) = qn(r)$ , we notice that  $T_{00}(r)/M - n(r) = \mathcal{O}(\alpha)$ . Therefore,  $\rho_{el}(r)$  (plotted in units of  $q/R^3$ ) and  $T_{00}(r)$  (plotted in units of  $M/R^3$ ) would not be distinguishable on the scale of Fig. 1a due to the numerical smallness of  $\alpha$ . However, the long-distance behaviors of the two distributions differ with  $T_{00}(r) \propto \frac{1}{r^4}$  while  $\rho_{el}(r) \propto \frac{1}{r^5}$  for  $r \gg R$ . As a consequence the mean radii defined as

$$\langle r_E^k \rangle = \frac{\int d^3r r^k T_{00}(r)}{M}, \quad \langle r_{\text{ch}}^k \rangle = \frac{\int d^3r r^k \rho_{\text{ch}}(r)}{q} \quad (14)$$

diverge for the energy distribution for  $k \geq 1$  and for the charge distribution for  $k \geq 2$ . Only the mean charge radius  $\langle r_{\text{ch}}^1 \rangle = 2R$  is finite.

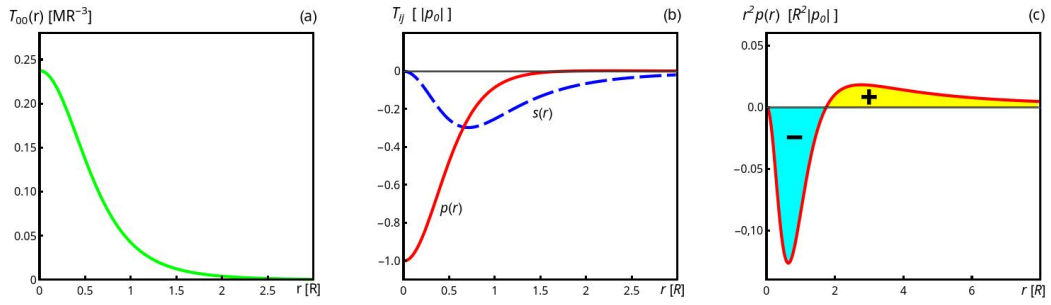


FIG. 1: Electron model EMT distributions as functions of  $r$  in units of electron radius  $R$ . (a) Energy distribution  $T_{00}(r)$  in units of  $M/R^3$ . (b) The stress tensor distributions  $s(r)$  and  $p(r)$  in units of  $|p_0|$ . (c) The distribution of  $r^2 p(r)$  in units of  $R^2 |p_0|$  illustrating how the von Laue condition in Eq. (16b) is satisfied. The sign patterns of the stress tensor distributions  $s(r)$  and  $p(r)$  are opposite to what has been found in hadronic models based on short-range interactions.

## B. The $T_{0k}$ components

The evaluation of the  $T_{0k}$  components of the EMT in Eq. (1) for the solutions (7, 8) yields  $T_{0k}(\vec{r}) = 0$ . The classical angular momentum  $J^i = \int d^3r \epsilon^{ijk} r^j T^{0k}$  of the system is therefore zero. Thus, in this toy model the “electron” appears to be spinless, although we shall find later an indication that the model is compatible with describing a spin- $\frac{1}{2}$  fermion rather than a spin zero boson (see Sec. IV). We remark that in principle one could try to explore projection techniques known from soliton physics [46] to assign spin quantum numbers to the classical solution. Note that spin effects were of no importance for the purposes of Ref. [32] and will also play no role in our study.

## C. The stress tensor $T_{ij}$

The static stress tensor  $T^{ij}$  of a spin-0 or spin- $\frac{1}{2}$  particle can be decomposed on general grounds into a traceless part and a trace described, respectively, in terms of the shear force  $s(r)$  and pressure  $p(r)$  distributions as follows

$$T^{ij}(\vec{r}) = \left( e_r^i e_r^j - \frac{1}{3} \delta^{ij} \right) s(r) + \delta^{ij} p(r). \quad (15)$$

EMT conservation implies the following two relations [11]

$$(a) \quad \frac{2}{3} s'(r) + \frac{2}{r} s(r) + p'(r) = 0, \quad (b) \quad \int_0^\infty dr r^2 p(r) = 0. \quad (16)$$

The latter is known as the von Laue condition and is a necessary (but not sufficient) condition for stability [47]. The computation of  $s(r)$  and  $p(r)$  in the model yields

$$s(r) = -\frac{1}{4\pi} E(r)^2 = -\frac{\alpha}{4\pi} \frac{r^2}{(r^2 + R^2)^3}, \quad (17)$$

$$p(r) = \frac{1}{24\pi} E(r)^2 - \lambda_p \kappa n(r)^{6/5} = \frac{\alpha}{24\pi} \frac{r^2}{(r^2 + R^2)^3} - \lambda_p \frac{\alpha}{8\pi} \frac{R^2}{(r^2 + R^2)^3}. \quad (18)$$

It can be readily checked analytically that the model results for  $s(r)$  and  $p(r)$  in Eqs. (17, 18) comply with the conditions in Eq. (16), which is an important internal consistency check for the model. The model results for the shear and pressure distributions are shown in Fig. 1b with  $s(r)$  and  $p(r)$  plotted in units of the modulus of  $p_0 = p(0)$ .

Notice that  $p_0 = -\frac{\alpha}{8\pi R^4}$  is negative and therefore can be expressed as  $p_0 = \frac{2E_{\text{bind}}}{\pi^2 R^3}$  with the (negative) binding energy  $E_{\text{bind}}$  in Eq. (12). Recall that pressure has the dimension of force/area or energy/volume, and the characteristic energy for stress tensor properties is the (in our case) negative binding energy. This is interesting. Another interesting observation is that  $s(r)$  and  $p(r)$  inside electron exhibit opposite signs to what have been observed in the interiors of hadrons in hadronic models based on short-range strong forces only (see the reviews [11, 12]). All patterns are the same as in hadronic models, except for the overall sign reversal. For instance, the shear force distribution is  $s(r) > 0$  for  $0 < r < \infty$  in hadronic models, but has the opposite sign in the electron model. Similarly, in hadronic models

$p(r) > 0$  is positive in the center of the particle and negative in the outer region, while in the electron model it is vice versa. In the electron model and others, the pressure exhibits a single node as is typical for ground state solutions and necessary to comply with the von Laue condition in Eq. (16b). The node of  $p(r)$  is located at  $r = \sqrt{3}R$  and difficult to see in Fig. 1b. We illustrate this feature and the compliance with the von Laue condition with more clarity by plotting  $r^2 p(r)$  in Fig. 1c.

At this point, we have no definite explanation for the reversed sign pattern of  $s(r)$  and  $p(r)$  in the electron model as compared to hadronic models. It is important to stress that the model describes the electron as a perfectly stable bound state as proven in [32]. However, the cohesive forces are introduced in this model by imposing the equation of state in Eq. (5) in an ad-hoc way, as has been criticized (by the same author!) in Ref. [36]. A possible explanation could therefore be that this is too simplistic a model with ad-hoc Poincaré stresses. A perhaps more plausible explanation might be that this effect is due to the long-range nature of electric forces. EMT properties different from those in hadrons have also been observed also in other systems governed by long-range forces [27–30].

However, our goal is not to investigate the “inner structure of the electron” in the experimentally unexplored region  $r \lesssim 10^{-20}$  m. Rather, our primary scope is to study the long-distance effects at distances  $r \gg R = 10^{-20}$  m. From the results in Eqs. (9, 17, 18) we read off the long-distance behavior of the EMT distributions

$$T_{00}(r) = \frac{\alpha}{8\pi} \frac{1}{r^4} + \dots, \quad s(r) = -\frac{\alpha}{4\pi} \frac{1}{r^4} + \dots, \quad p(r) = \frac{\alpha}{24\pi} \frac{1}{r^4} + \dots \quad (19)$$

where the dots indicate subleading terms decaying at large distances like  $\frac{1}{r^5}$  or faster. The results in Eq. (19) agree with Ref. [22–26] and offer a “mathematical” explanation of the reversed sign pattern as follows.

For  $r \gg R$ , the model must (and does) reproduce the electric field of a pointlike charge with the electrostatic energy density  $T_{00}(r) = \frac{1}{8\pi} \vec{E}^2$  and Maxwell stress tensor  $T_{ij}(r) = -\frac{1}{4\pi} (E_i E_j - \frac{1}{2} \delta_{ij} \vec{E}^2)$  which also yields Eq. (19). Thus, the signs at asymptotically large distances are dictated by Maxwell’s theory of electromagnetism and there must be no modification to the model in the far region. Modifications can occur only in the model-dependent near region, and since  $p(r)$  must have a node somewhere (in the near region) to comply with the von Laue condition (16b), one is inevitably lead to the sign pattern of  $p(r)$  in Fig. 1. The sign pattern of  $s(r)$  then follows from Eq. (16a). In the next section, we will discuss the consequences for the EMT form factors due to the long-distance behavior of the EMT distributions in Eq. (19).

#### IV. THE EMT FORM FACTORS $A(t)$ AND $D(t)$

The matrix elements of the total symmetric EMT operator  $\hat{T}^{\mu\nu}$  of a quantum particle (in the absence of parity violating interactions) define the EMT form factors as [2, 48]

$$\langle p' | \hat{T}^{\mu\nu} | p \rangle = \bar{u}(p', s') \left[ A(t) \frac{P^\mu \gamma^\nu + P^\nu \gamma^\mu}{2} + B(t) \frac{i(P^\mu \sigma^{\nu\rho} + P^\nu \sigma^{\mu\rho}) \Delta_\rho}{4M} + D(t) \frac{\Delta^\mu \Delta^\nu - g^{\mu\nu} \Delta^2}{4M} \right] u(p, s), \quad (20)$$

where  $P = \frac{1}{2}(p + p')$  and  $\Delta = p' - p$ . The spinor normalization is  $\bar{u}(p, s') u(p, s) = 2M \delta_{ss'}$  and the general constraints  $A(0) = 1$  and  $B(0) = 0$  hold due to Lorentz invariance. For particles whose size  $R$  is much larger than their Compton wavelength  $\lambda_c \gg 1/M$ , i.e.  $RM \gg 1$ , the Fourier transform of the EMT matrix elements in the Breit frame where  $p^\mu = (E, -\frac{1}{2}\vec{\Delta})$  and  $p'^\mu = (E, \frac{1}{2}\vec{\Delta})$  gives rise to spatial distributions according to the interpretation [10]

$$T^{\mu\nu}(\vec{r}) = \int \frac{d^3\Delta}{2E(2\pi)^3} \langle p', s' | \hat{T}^{\mu\nu} | p, s \rangle e^{-i\vec{\Delta} \cdot \vec{r}}. \quad (21)$$

In classical models, the spatial distributions can be exactly computed, and form factors are obtained from inverting the Fourier transforms [23, 24].  $D(t)$  can be obtained in two different ways: from  $s(r)$  and  $p(r)$ , which we denote as  $D_s(t)$  and  $D_p(t)$  and which must coincide.  $A(t)$  is determined in a unique way. The expressions are given by [49–51]

$$D_s(t) = 4M \int d^3r \frac{j_2(r\sqrt{-t})}{t} s(r), \quad D_p(t) = 6M \int d^3r \frac{j_0(r\sqrt{-t})}{t} p(r), \quad (22)$$

$$A(t) = \frac{1}{M} \int d^3r j_0(r\sqrt{-t}) T_{00}(r) - \frac{t}{4M^2} (B(t) - D(t)), \quad (23)$$

where  $j_i(x)$  are spherical Bessel functions.

The Compton wavelength of the electron is much larger than its experimentally known upper bound for its size, and the condition  $RM \gg 1$  is not satisfied. In such a situation, one could argue that one may assume  $RM \gg 1$  during

the calculation before taking the limit to realistic values. However, with our focus remaining on analytical results, we are not going to insert the numerical values anyway. Evaluating the expressions for  $D(t)$  in the model, we obtain

$$\begin{aligned} D_s(t) &= \frac{\alpha \pi M}{4} e^{-R\sqrt{-t}} \frac{1}{\sqrt{-t}} \\ D_p(t) &= \frac{\alpha \pi M}{4} e^{-R\sqrt{-t}} \left[ \frac{3(1-\lambda_p)}{4Rt} + \frac{(3\lambda_p+1)}{4\sqrt{-t}} \right]. \end{aligned} \quad (24)$$

$D_s(t)$  arises solely from the electric contribution, while  $D_p(t)$  arises from both electric forces and Poincaré stresses. Recalling that  $\lambda_p$  is unity (see Eq. (10)), we obtain the same expression  $D(t) = D_s(t) = D_p(t)$  from either method as expected, which constitutes another theoretical consistency test of the model. Expanding  $D(t)$  around  $t = 0$  yields

$$D(t) = \frac{\alpha \pi}{4} \frac{M}{\sqrt{-t}} - \frac{\alpha \pi}{4} R M + \dots \quad (25)$$

The leading term in Eq. (25) is model independent and agrees with the QED result [26]. The subleading terms are model dependent as can be seen from the appearance of the model parameter  $R$ . The dots in Eq. (25) indicate terms proportional to  $\sqrt{-t}$  and higher powers thereof. In small- $t$  expansion of  $D(t)$  in QED a term  $\ln \sqrt{-t}$  appears at subleading order [26], which does not appear in the model.

In order to compute  $A(t)$  in Eq. (23) we need, in addition to  $T_{00}(r)$  and  $D(t)$  (which are known in the model), the form factor  $B(t) = A(t) - 2J(t)$  where  $J(t)$  is the EMT form factor associated with total angular momentum (which is not known in the model, see Sec. III B). Since  $B(t)$  vanishes at  $t = 0$  and moreover enters in Eq. (23) with a prefactor of  $t$ , this contribution becomes relevant for  $A(t)$  in Eq. (23) only beyond  $\mathcal{O}(t)$  and can be safely neglected if we study  $A(t)$  in the small- $t$  region. The computation of  $B(t)$  is beyond the capability of the present model.

Evaluating the Fourier transform of  $T_{00}(r)$  in Eq. (23) and combining with the result for  $D(t)$  from  $s(r)$  in Eq. (24) (where no  $\lambda_p$  appears) yields the following result

$$A(t) = \alpha \pi \left[ \frac{3-5\lambda_p}{32MR} - \frac{(3+5\lambda_p)\sqrt{-t}}{32M} \right] e^{-R\sqrt{-t}} + \frac{m_{\text{fluid}}}{M} \left[ R\sqrt{-t} K_1(R\sqrt{-t}) \right] + \frac{tB(t)}{4M^2}, \quad (26)$$

where  $K_n(z)$  is the modified Bessel function of the second kind for  $n = 1$ . Expanding this result around  $t = 0$  with  $\sqrt{z} K_1(\sqrt{z}) = 1 + \frac{1}{4}z(\ln z + 2\gamma - 1 - 2\ln 2) + \mathcal{O}(z^{3/2})$ , where  $\gamma$  is the Euler-Mascheroni constant, yields

$$A(t) = 1 - \frac{3\pi\alpha}{16} \frac{\sqrt{-t}}{M} - \frac{m_{\text{fluid}}}{2M} R^2 t \ln\left(\frac{1}{2}R\sqrt{-t}\right) + \dots \quad (27)$$

where the dots indicate terms of  $\mathcal{O}(t)$ . We made use of Eq. (11) to simplify the coefficients of the first two terms. The model complies with the general constraint  $A(0) = 1$ . The first non-trivial term in Eq. (25) proportional to  $\sqrt{-t}$  corresponds exactly to the QED result [26]. We see that the model generates a subleading logarithmic term in  $A(t)$  as in QED [26] but with a different, model-dependent coefficient. Higher order terms are also model dependent.

It is also instructive to consider the small  $R$  limit. Expanding the model expressions in Eqs. (24, 26) at fixed  $t$  for small  $R$  yields the results

$$A(t) = 1 - \frac{3\pi\alpha}{16} \frac{\sqrt{-t}}{M} \left\{ 1 + \mathcal{O}(\epsilon \ln \epsilon) \right\}, \quad D(t) = \frac{\alpha\pi}{4} \frac{M}{\sqrt{-t}} \left\{ 1 + \mathcal{O}(\epsilon) \right\}, \quad \epsilon = R\sqrt{-t}. \quad (28)$$

For  $A(t)$ , we used Eq. (11) and  $m_{\text{fluid}} = \mathcal{O}(\frac{\epsilon}{R})$  which follows from the discussion below Eq. (13). In the limit  $R \rightarrow 0$  the  $\frac{1}{R}$  singularity in the electron mass  $M$  is compensated by the ‘‘counter term’’  $m_{\text{fluid}}$ , which reflects the renormalization of the electron mass due to short-distance (UV) effects in QED. The small- $R$  limit mimics the restoration of a point-like particle in the model. The results in Eq. (28) demonstrate that we can derive model-independently the leading terms in Eqs. (25, 27), but not higher order terms.

Next we consider the limit of a point-like, free particle, which can be carried out by taking in Eq. (28) the limit  $R \rightarrow 0$  followed by taking the electromagnetic coupling constant  $\alpha \rightarrow 0$ . The result is trivial

$$A(t) = 1, \quad D(t) = 0. \quad (29)$$

For point-like, free particles one expects constant form factors [52, 53]. Since  $A(0) = 1$  must hold in any (free or interacting) theory, one must expect  $A(t) = 1$  for point-like, non-interacting particles of all types which we obtain. For  $D(t)$  the situation is different because the result depends on particle type, e.g., one has  $D(t) = 1$  for a free spin-0

boson [52], and  $D(t) = 0$  for a free spin- $\frac{1}{2}$  fermion [53]. Our result in Eq. (28) is compatible with the  $D(t)$  of a free spin- $\frac{1}{2}$  fermion which indicates that this model really describes an electron, even though the explicit description of spin degrees of freedom (if possible in this framework) would require additional effort (see Sec. III B).

For completeness, we note that for large  $(-t)$ , the model form factors in Eqs (24, 26) decay exponentially and  $\lim_{t \rightarrow -\infty} A(t)/D(t) = -1$ . This differs from QED [26] and is expected as this limit is beyond the reach of classical models. Notice that with increasing  $(-t)$  QED is eventually superseded by the electroweak theory. For discussions of EMT properties in electroweak theory for Higgs and  $Z$ -bosons, we refer to Ref. [54].

## V. COMMENTS ON PROTON $D$ -TERM REGULARIZATION OF REFS. [23, 24]

The leading  $1/\sqrt{|t|}$ -term in Eqs. (25, 28) is a universal QED effect which implies that  $D$ -terms of charged particles are divergent and undefined. In Refs. [23, 24] it was proposed that for the proton it makes sense to introduce a “regularization” to define a finite, regularized value  $D_{\text{reg}}$  of the  $D$ -term for the following reason. The proton is an extended particle and the shape of its  $D(t)$  is strongly dominated by the strong forces in the experimentally accessible  $t$ -region, and QED effects become noticeable only for  $(-t) \ll 10^{-4} \text{ GeV}^2$  which cannot be accessed in experiments in the foreseeable future [23, 24]. In contrast to the proton, in the case of the electron the concept of a regularized  $D$ -term is not physically justified. However, it is interesting to explore the exactly solvable electron model to give insights on how this regularization method works.

The regularization method [24] works as follows. Let  $F(r)$  be a 3D distribution related to the stress tensor, and let the integral  $I_n = \int d^3r r^n F(r)$  be divergent due to the long-range em forces. We define a regularized integral by

$$I_{n,\text{reg}} = \int d^3r r^n F(r)_{\text{reg}} = \int d^3r r^n \left[ F(r) + Z_F \left\{ \frac{2}{3} n s(r) + (n+3) p(r) \right\} \right], \quad Z_F = \lim_{r \rightarrow \infty} \frac{r^4 F(r)}{\frac{1}{2}(n-1) \frac{\alpha}{4\pi}}, \quad (30)$$

where the added term in the curly brackets originates from the identity  $\frac{2}{3}s'(r) + \frac{2}{r}s(r) + p'(r) = 0$  with the quoted expression following after an integration by parts. The coefficient  $Z_F$  in Eq. (30) is defined in such a way that the integral  $I_n$  becomes finite. Let us apply this method first to the  $D$ -term.

Taking the limit  $t \rightarrow 0$  in Eq. (22) yields the expressions  $D_s = -\frac{4}{15} M \int d^3r r^2 s(r)$  and  $D_p = M \int d^3r r^2 p(r)$  which are both divergent due to the long-distance behavior of the distributions in Eq. (19). Applying the regularization method in Eq. (30) we obtain from  $D_s$  and  $D_p$  the unambiguous result

$$D_{\text{reg}} = -\lambda_p \frac{\alpha \pi}{4} MR. \quad (31)$$

Several comments are in order. First, the regularization works and “removes” the divergence due to electromagnetic effects leaving behind a finite, and negative value for the regularized  $D$ -term. Second, the appearance of  $\lambda_p$  signals that the result is due to the Poincaré stresses. This is in line with results from models based on short-range forces where the  $D$ -terms are finite, negative, and their negative signs can be traced back to the forces binding the system. Third, comparing the small- $t$  expansion of  $D(t)$  in the model in Eq. (25) and the result in Eq. (31) and recalling that  $\lambda_p = 1$ , we see what the regularization method did: it removed the first, divergent term in Eq. (25) which is of electromagnetic origin and retained the second, finite term which originates from the Poincaré stresses.

As a second example we consider the mechanical radius which is defined in terms of the normal force per unit area  $p_n(r) = \frac{2}{3}s(r) + p(r)$  as follows

$$\langle r_{\text{mech}}^2 \rangle = \frac{\int d^3r r^2 p_n(r)}{\int d^3r p_n(r)}. \quad (32)$$

In models based on short range forces the distribution  $p_n(r)$  is positive definite, making the definition (32) a meaningful proxy for particle size. In the electron model, the  $p_n(r)$  is negative and the numerator in Eq. (32) is divergent at large- $r$  due to the long-distance asymptotics in Eq. (19). Remarkably, the regularization prescription fixes both issues since

$$[p_n(r)]_{\text{reg}} = \frac{\alpha}{2\pi} \frac{\lambda_p R^2}{(r^2 + R^2)^3} \geq 0, \quad \langle r_{\text{mech}}^2 \rangle = \frac{\int d^3r r^2 [p_n(r)]_{\text{reg}}}{\int d^3r [p_n(r)]_{\text{reg}}} = 3\lambda_p R^2. \quad (33)$$

Note that both the numerator and denominator in Eq. (33) explicitly depend on  $\lambda_p$ . Thus, it is the Poincaré stress that gives the electron in this model a mechanical radius within the regularization procedure of Eq. (30).

We stress that it is not our intention to define a regularized  $D$ -term for the electron. But for the proton it arguably makes sense to introduce a  $D_{\text{reg}}$  for practical purposes [23, 24], and our investigation shows how this regularization method works: it removes the electromagnetic contribution from  $D$  and leaves behind a negative contribution from internal binding forces.

## VI. CONCLUSIONS

We have carried out a study of the EMT properties of the electron in a lucid classical model by Białynicki-Birula [32]. In this model, the electron is made of a charged ideal fluid, electric forces and imposed Poincaré stresses designed to overcome the electrostatic repulsion in the fluid and yield a stable bound state. The parameters in the model can in principle be fixed such that the system has the mass  $M$  of the electron and the size  $R = 10^{-20}$  m within experimental limits of the electron radius. However, the model can be solved exactly and the parameters  $M$  and  $R$  can be left general in all steps. The description of spin degrees of freedom is beyond the scope of this model.

In classical frameworks, one can compute exactly the EMT 3D spatial distributions. The obtained model results are very interesting. The positive definite energy distribution  $T_{00}(r)$  does not indicate anything unusual, but the distributions associated with the stress tensor exhibit exactly the opposite sign patterns to what is found in hadronic models governed by short-range strong forces only. We have shown that from a mathematical point of view, this is an inevitable consequence of the fact that at large distances  $r \gg R$  the model must reproduce the results from (classical or quantized) Maxwell theory of electromagnetism, which is the case. More work may be needed to understand the underlying physical reasons. Ultimately, the reversed sign pattern is related to the masslessness of the photon and the long-range character of the electromagnetic interaction.

In quantum frameworks, one may compute form factors and interpret them in terms of 3D spatial densities in systems where the particle's size is large compared to the particle's Compton wavelength which requires  $MR \gg 1$ . For the electron this condition is not met. However, in our analytically carried out calculation we may, for instance, assume that  $MR$  is kept large throughout the calculation, and invert the Fourier transforms in the quantum interpretation to compute form factors from exactly known, classical 3D distributions. The results are insightful. We have shown that the model complies with the general constraint  $A(0) = 1$  for the form factor  $A(t)$  and moreover reproduces the leading non-analytic terms of  $A(t)$  and  $D(t)$ , which are proportional to respectively  $\sqrt{-t}$  and  $1/\sqrt{-t}$  with correct coefficients that coincide with QED [25, 26]. This supports the validity of the model results obtained for the EMT form factors in the small- $(-t)$  region. One remarkable result is that in the limit of a point-like, non-interacting particle one obtains in the model  $D(t) = 0$  which corresponds to a free spin  $\frac{1}{2}$ -fermion.

As an application of this lucid model, we presented the investigation of the concept of a regularized proton  $D$ -term [23]. This concept is motivated by the fact that for the proton the QED divergence in  $D(t) \sim 1/\sqrt{-t}$  is noticeable only for  $(-t) \ll 10^{-4} \text{GeV}^2$  beyond the reach of experiments [24], and one will see  $D(t)_{\text{prot}} \approx D_{\text{prot,reg}}/(1 + t/m_D^2)^{n_D}$  with some parameters  $m_D$  and  $n_D$  in the experimentally accessible region. In the proton case, the regularization is designed to “remove” the electromagnetic contribution to  $D(t)$  without affecting the strong interaction contributions responsible for the binding effects as can be inferred from a comparison to the neutron [24].

In the electron case, the concept of a regularized  $D$ -term is not justified. However, it is interesting to use the model to see how this regularization works. In fact, in the model the stress tensor distributions defining the  $D$ -term receive contributions from electric forces and Poincaré stresses, and the regularization removes only the former leaving behind a result which is (i) finite, (ii) negative, and (iii) due to the Poincaré stresses which bind the system. This is in line with results from hadronic models based on short range forces only where one also finds a  $D$ -term which is (i) finite, (ii) negative, and (iii) the sign of the  $D$ -term is ultimately due to the forces which bind the system [49].

It would be interesting to investigate whether a classical model can be constructed which is also capable of reproducing subleading terms in the small- $t$  expansion of the EMT form factors in QED. Another interesting question is whether there is a way to include spin degrees of freedom. These topics will be left to future studies.

**Acknowledgments.** The authors wish to thank Adam Freese, Barbara Pasquini and Simone Rodini for valuable discussions. This work was supported by the National Science Foundation under the Award No. 2412625, and DOE under the umbrella of the Quark-Gluon Tomography (QGT) Topical Collaboration with Award No. DE-SC0023646.

- 
- [1] X. D. Ji, Phys. Rev. D **52**, 271-281 (1995) [arXiv:hep-ph/9502213 [hep-ph]].
  - [2] X. D. Ji, Phys. Rev. Lett. **78**, 610 (1997), [hep-ph/9603249].
  - [3] M. V. Polyakov and C. Weiss, Phys. Rev. D **60**, 114017 (1999) [arXiv:hep-ph/9902451 [hep-ph]].
  - [4] X. D. Ji, J. Phys. G **24**, 1181 (1998).
  - [5] A. V. Radyushkin, arXiv:hep-ph/0101225.
  - [6] K. Goeke, M. V. Polyakov and M. Vanderhaeghen, Prog. Part. Nucl. Phys. **47**, 401 (2001).
  - [7] M. Diehl, Phys. Rept. **388** (2003) 41.
  - [8] A. V. Belitsky and A. V. Radyushkin, Phys. Rept. **418**, 1 (2005).
  - [9] S. Boffi and B. Pasquini, Riv. Nuovo Cim. **30**, 387 (2007).
  - [10] M. V. Polyakov, Phys. Lett. B **555**, 57 (2003) [hep-ph/0210165].

- [11] M. V. Polyakov and P. Schweitzer, *Int. J. Mod. Phys. A* **33**, 1830025 (2018) [arXiv:1805.06596 [hep-ph]].
- [12] V. D. Burkert, L. Elouadrhiri, F. X. Girod, C. Lorcé, P. Schweitzer and P. E. Shanahan, *Rev. Mod. Phys.* **95**, 041002 (2023) [arXiv:2303.08347 [hep-ph]].
- [13] C. Lorcé, H. Moutarde and A. P. Trawiński, *Eur. Phys. J. C* **79**, no.1, 89 (2019) [arXiv:1810.09837 [hep-ph]].
- [14] A. Freese and G. A. Miller, *Phys. Rev. D* **103**, 094023 (2021) [arXiv:2102.01683 [hep-ph]].
- [15] C. Lorcé and P. Schweitzer, *Acta Phys. Polon. B* **56**, 3-A17 (2025) [arXiv:2501.04622 [hep-ph]].
- [16] G. A. Miller, *Phys. Rev. C* **112**, 045204 (2025) [arXiv:2507.14388 [hep-ph]].
- [17] X. Ji and C. Yang, *Nucl. Phys. B* **1024**, 117342 (2026) [arXiv:2508.16727 [hep-ph]].
- [18] R. Hofstadter, *Rev. Mod. Phys.* **28**, 214-254 (1956).
- [19] F. A. Berends and R. Gastmans, *Annals Phys.* **98**, 225 (1976).
- [20] K. A. Milton, *Phys. Rev. D* **15**, 538 (1977).
- [21] B. Kubis and U. G. Meissner, *Nucl. Phys. A* **671**, 332 (2000); *ibid. A* **692**, 647 (2001)
- [22] J. F. Donoghue, B. R. Holstein, B. Garbrecht and T. Konstandin, *Phys. Lett. B* **529**, 132-142 (2002) [erratum: *Phys. Lett. B* **612**, 311-312 (2005)] [arXiv:hep-th/0112237 [hep-th]].
- [23] M. Varma and P. Schweitzer, *Phys. Rev. D* **102**, 014047 (2020) [arXiv:2006.06602 [hep-ph]].
- [24] A. Mejia and P. Schweitzer, *Phys. Rev. D* **113**, 054016 (2026) [arXiv:2511.21916 [hep-ph]].
- [25] A. Metz, B. Pasquini and S. Rodini, *Phys. Lett. B* **820**, 136501 (2021) [arXiv:2104.04207 [hep-ph]].
- [26] A. Freese, A. Metz, B. Pasquini and S. Rodini, *Phys. Lett. B* **839**, 137768 (2023) [arXiv:2212.12197 [hep-ph]].
- [27] J. Y. Panteleeva, *Phys. Rev. D* **107**, 055015 (2023) [arXiv:2302.11980 [hep-ph]].
- [28] X. Ji, J. Yang and Y. Liu, *Phys. Rev. D* **110**, 114045 (2024) [arXiv:2208.05029 [hep-ph]].
- [29] A. Czarnecki, Y. Liu and S. N. Reza, *Acta Phys. Polon. Supp.* **16**, 7-A19 (2023) [arXiv:2309.10994 [hep-ph]].
- [30] A. Freese, *Phys. Rev. D* **111**, 034047 (2025) [arXiv:2412.09664 [hep-ph]].
- [31] J. J. Thomson, *The Electrician*, **39**, 104–109 (1897); *Phil. Mag. Ser. 5* **44**, 293-316 (1897).
- [32] I. Białynicki-Birula, *Phys. Rev. D* **28**, 2114-2117 (1983).
- [33] P. A. Dirac, *Proc. Roy. Soc. Lond. A* **268**, 57 (1962).
- [34] J. S. Schwinger, *Found. Phys.* **13**, 373 (1983).
- [35] P. Pearle, “Classical Electron Models in Electromagnetism,” Chapter 7 in “Paths to Research”, Ed. D. Teplitz, (Plenum, New York, 1982).
- [36] I. Białynicki-Birula, *Phys. Lett. A* **182** (1993), 346-352 [arXiv:nucl-th/9306006 [nucl-th]].
- [37] F. Rohrlich, *Am. J. Phys.* **65** (1997), 1051-1056.
- [38] T. H. Boyer, *Phys. Rev. D* **25**, 3246-3250 (1982).
- [39] F. Rohrlich, *Phys. Rev. D* **25**, 3251-3255 (1982)
- [40] H. Poincaré, *Rendiconti del Circolo Matematico di Palermo* **21**, 129 (1906).
- [41] S. J. Brodsky and S. D. Drell, *Phys. Rev. D* **22**, 2236 (1980).
- [42] H. Dehmelt, *Rev. Mod. Phys.* **62**, 525-530 (1990).
- [43] G. Kopp, D. Schaile, M. Spira and P. M. Zerwas, *Z. Phys. C* **65**, 545-550 (1995) [arXiv:hep-ph/9409457 [hep-ph]].
- [44] M. Acciarri *et al.* [L3], *Phys. Lett. B* **489**, 81-92 (2000) [arXiv:hep-ex/0005028 [hep-ex]].
- [45] M. E. Peskin, [arXiv:2003.05435 [hep-ph]].
- [46] R. Rajaraman, “Solitons and Instantons Amsterdam,” (North-Holland, Amsterdam, 1982).
- [47] M. Laue, *Annalen Phys.* **340**, 524-542 (1911).
- [48] I. Y. Kobzarev and L. B. Okun, *Zh. Eksp. Teor. Fiz.* **43**, 1904 (1962) [*Sov. Phys. JETP* **16**, 1343 (1963)].  
H. Pagels, *Phys. Rev.* **144**, 1250 (1966).
- [49] K. Goeke, J. Grabis, J. Ossmann, M. V. Polyakov, P. Schweitzer, A. Silva and D. Urbano, *Phys. Rev. D* **75**, 094021 (2007).
- [50] K. Goeke, J. Grabis, J. Ossmann, P. Schweitzer, A. Silva and D. Urbano, *Phys. Rev. C* **75**, 055207 (2007).
- [51] C. Cebulla, K. Goeke, J. Ossmann and P. Schweitzer, *Nucl. Phys. A* **794**, 87-114 (2007) [arXiv:hep-ph/0703025 [hep-ph]].
- [52] J. Hudson and P. Schweitzer, *Phys. Rev. D* **96**, 114013 (2017).
- [53] J. Hudson and P. Schweitzer, *Phys. Rev. D* **97**, 056003 (2018).
- [54] P. Beißner, B. D. Sun, E. Epelbaum and J. Gegelia, *Eur. Phys. J. C* **85**, 1471 (2025) [arXiv:2508.19821 [hep-ph]].  
P. Beißner, J. Y. Panteleeva, B. D. Sun, E. Epelbaum and J. Gegelia, [arXiv:2601.22731 [hep-ph]].